Available online at www.sciencedirect.com
ScienceDirect
Journal of Solid State Chemistry 180 (2007) 1882–1888
JOURNAL OF SOLID STATE CHEMISTRY
www.elsevier.com/locate/jssc

Composition-induced phase transition in $Ca_{14}Zn_{6-x}Ga_{10+x}O_{35+x/2}$ ($x = 0.0$ and 0.5)

S.Ya. Istomin[a,*], S.V. Chernov[b], E.V. Antipov[a], Yu.A. Dobrovolsky[b]

[a]*Department of Chemistry, Moscow State University, 119992 Moscow, Russia*
[b]*Institute of Problems of Chemical Physics, RAS, 142432, Acad. Semenov av., 1, Chernogolovka, Moscow Region, Russia*

Received 12 December 2006; received in revised form 24 April 2007; accepted 25 April 2007
Available online 1 May 2007

Abstract

Novel complex oxides $Ca_{14}Zn_6Ga_{10}O_{35}$ and $Ca_{14}Zn_{5.5}Ga_{10.5}O_{35.25}$ were prepared in air at 1200 °C, 72 h. Refinements of their crystal structures using X-ray powder diffraction data showed that $Ca_{14}Zn_6Ga_{10}O_{35}$ is ordered (S.G. $F23$, $R_F^2 = 0.0458$, $R_p = 0.0485$, $R_{wp} = 0.0659$, $\chi^2 = 1.88$) and $Ca_{14}Zn_{5.5}Ga_{10.5}O_{35.25}$ disordered (S.G. $F432$, $R_F^2 = 0.0346$, $R_p = 0.0601$, $R_{wp} = 0.0794$, $\chi^2 = 2.82$) variants of the crystal structure of $Ca_{14}Zn_6Al_{10}O_{35}$. In the crystal structure of $Ca_{14}Zn_6Ga_{10}O_{35}$, there are large empty voids, which could be partially occupied by additional oxygen atoms upon substitution of Zn^{2+} by Ga^{3+} as in $Ca_{14}Zn_{5.5}Ga_{10.5}O_{35.25}$. These oxygen atoms are introduced into the crystal structure of $Ca_{14}Zn_{5.5}Ga_{10.5}O_{35.25}$ only as a part of four tetrahedra (Zn, Ga)O_4 groups sharing common vertex. This creates a situation where even a minor change in the chemical composition leads to considerable anion and cation disordering resulting in a change of space group from $F23$ (no. 196) to $F432$ (no. 209).

Keywords: $Ca_{14}Zn_6Ga_{10}O_{35}$; X-ray powder diffraction; Crystal structure

1. Introduction

Search for novel fast oxide-ion conductors, which in the future could replace Y-doped zirconia as electrolyte in solid oxide fuel cells (SOFC), remains one of the important tasks for the researchers working in the field of solid state chemistry. From the viewpoint of crystallochemistry, one of the criteria in the search of novel oxide-ion conductors is a crystal structure with large empty voids, which could be partially filled by oxide ions upon appropriate cation substitution.

Recently, complex cobaltites $Ca_7Co_3Ga_5O_{18}$ [1] and manganites $Ca_{6.3}Mn_3Ga_{4.4}Al_{1.3}O_{18}$ [2] crystallizing in a large F-centered cubic structure ($F432$, no. 209) with $a \approx 15$ Å were synthesized. Their crystal structures represent disordered variants of the $Ca_{14}Zn_6Al_{10}O_{35}$ structure [3] and can be described as 3D-frameworks of corner-shared tetrahedra inside which isolated MO_6 octahedra (M = Co, Mn), surrounded by eight Ca atoms, are located. In the ordered $Ca_{14}Zn_6Al_{10}O_{35}$ (S.G. $F23$, no. 196) structure large empty voids are present. These empty voids can be partly filled with groups of four vertex-linked tetrahedra sharing a common oxygen atom in the center as in the case of $Ca_7Co_3Ga_5O_{18}$ and $Ca_{6.3}Mn_3Ga_{4.4}Al_{1.3}O_{18}$. This leads to substantial cation and anion disorder in their crystal structures [1,2].

In the present paper, we report on the crystal structures of the novel compounds $Ca_{14}Zn_6Ga_{10}O_{35}$ and $Ca_{14}Zn_{5.5}Ga_{10.5}O_{35.25}$. The structural refinement using X-ray powder diffraction data revealed them to have an ordered and disordered variant of the $Ca_{14}Zn_6Al_{10}O_{35}$-related crystal structures and that already a minute change of the chemical composition leads to change of space group from $F23$ to $F432$.

2. Experimental

$Ca_{14}Zn_{6-x}Ga_{10+x}O_{35+x/2}$, $-0.5 \leqslant x \leqslant 1$ ($\Delta x = 0.5$) samples were prepared from stoichiometric amounts of ZnO, Ga_2O_3 and $CaCO_3$ annealed in air at 1200 °C for 72 h.

*Corresponding author. Fax: +7 495 9394788.
E-mail address: istomin@icr.chem.msu.ru (S.Ya. Istomin).

0022-4596/$ - see front matter © 2007 Elsevier Inc. All rights reserved.
doi:10.1016/j.jssc.2007.04.013

Phase analysis was performed by means of their X-ray powder diffraction (XRD) patterns recorded in a Huber G670 Guinier diffractometer (Cu$K\alpha_1$ radiation, image plate detector). The crystal structures of $Ca_{14}Zn_6Ga_{10}O_{35}$ and $Ca_{14}Zn_{5.5}Ga_{10.5}O_{35.25}$ were refined using the GSAS [4] program suite and X-ray diffraction data collected with a STADI-P (STOE), Cu$K\alpha_1$, $\lambda = 1.54060$ Å.

For the electrical characterization of the materials, powders of the $Ca_{14}Zn_6Ga_{10}O_{35}$ and $Ca_{14}Zn_{5.5}Ga_{10.5}O_{35.25}$ were pressed into pellets of 6 mm of diameter and 2 mm of thickness. The resulting pellets were sintered in air at 1230 °C, 5 h. Pt-paste (Heraeus OS2) was painted on both sides of the pellets and fired at 950 °C for 15 min. The impedance spectroscopy measurements were performed on Z-350 M (Elins) impedance analyzer in air and in Ar/air mixture ($P_{O_2} = 1.6 \times 10^{-4}$–0.015 atm) in the 5 kHz to 1 MHz frequency range from 725 to 935 °C. Data were analyzed using the ZView v2.8 program [5].

3. Results

Single-phase samples were obtained only for the compositions with $x = 0$ (white color) and 0.5 (light yellow). The XRD patterns of both samples could be indexed with F-centered cubic unit cells, although with slightly different unit cell parameters (Table 1). In the XRD patterns of the $x = -0.5$ and 1.0 samples additional reflections from unidentified phases were present.

Careful examination of the XRD patterns revealed the intensity distribution between the reflections at low 2θ angles to be quite different for the compounds, as shown in Fig. 1. This indicated significant structural changes upon small compositional changes. For example, the intensity ratio of the reflections (311) and (222) increases from $I_{(311)}/I_{(222)} = 1.8$ to 2.5 upon doping. One explanation for such a result could be preferred orientation. However, the allowances of preferred orientation in the structural refinements of both compounds did not improve the results. As the crystal structures of $Ca_{14}Zn_6Ga_{10}O_{35}$ and $Ca_{14}Zn_{5.5}Ga_{10.5}O_{35.25}$ were refined using X-ray powder diffraction data, it was not possible to distinguish between Zn ($Z = 30$) and Ga ($Z = 31$). The scattering power of Zn was therefore used for both positions. The use of X-rays also leads to problem with the precision of the oxygen atom positions. This also made it necessary to use common atomic displacement parameters (ADP) for the oxygen atoms in the refinements.

Table 1
Phase analysis data for the $Ca_{14}Zn_{6-x}Ga_{10+x}O_{35-x/2}$ samples prepared at 1200 °C

x-Value	Unit cell parameters (Å)	Admixtures
−0.5	15.0856(6)	Yes (maximum $I \approx 5\%$)
0.0	15.0838(4)	–
0.5	15.0632(9)	–
1.0	15.0592(5)	Yes (maximum $I \approx 12\%$)

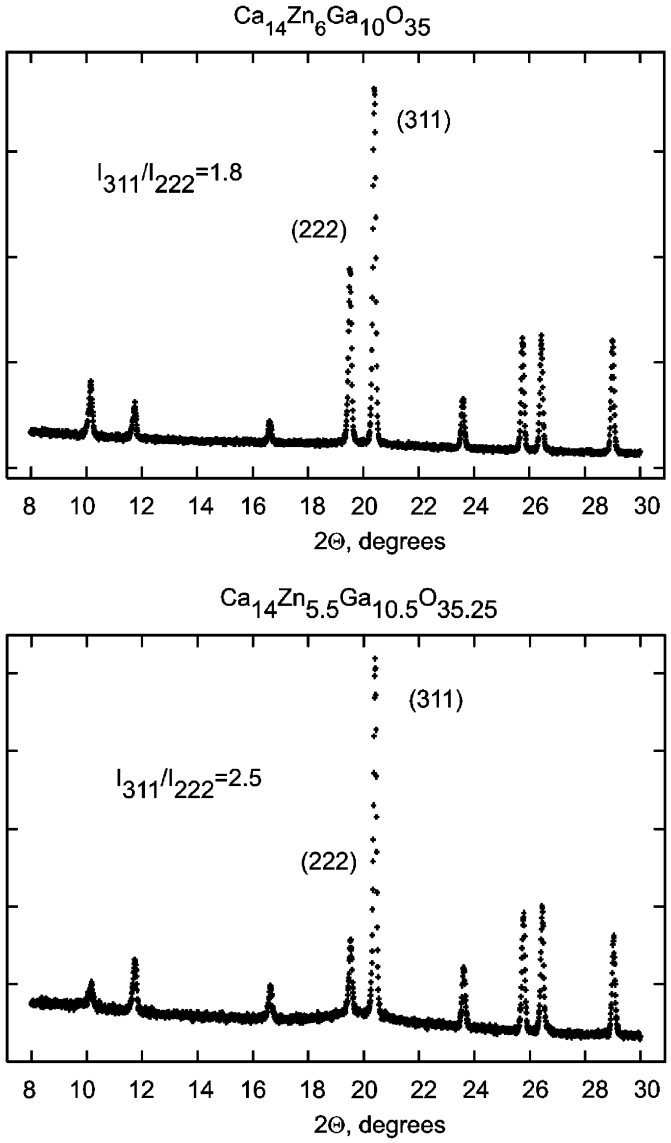

Fig. 1. Part of the X-ray powder diffraction patterns of $Ca_{14}Zn_6Ga_{10}O_{35}$ and $Ca_{14}Zn_{5.5}Ga_{10.5}O_{35.25}$. Note the significant different intensity distribution between the samples for some reflections at low angles.

Two models 1 and 2 were tested in the refinements of the crystal structures. Model 1 was ordered model of $Ca_{14}Zn_6Al_{10}O_{35}$ [3] in space group $F23$ while model 2 was based on the disordered structure of $Ca_7Co_3Ga_5O_{18}$ [1], space group $F432$.

3.1. The crystal structure of $Ca_{14}Zn_6Ga_{10}O_{35}$

Refinement of the crystal structure of $Ca_{14}Zn_6Ga_{10}O_{35}$ in model 2 resulted in high reliability factors of $\chi^2 = 12.0$, $R_F^2 = 0.090$, $R_p = 0.0764$ and physically meaningless ADPs, while the refinement in the ordered model 1 converged smoothly. Crystal data, atomic coordinates and ADPs are presented in Tables 2 and 3, respectively. Selected interatomic distances are given in Table 4.

Table 2
Crystal data for $Ca_{14}Zn_6Ga_{10}O_{35}$ and $Ca_{14}Zn_{5.5}Ga_{10.5}O_{35.25}$

	$Ca_{14}Zn_6Ga_{10}O_{35}$	$Ca_{14}Zn_{5.5}Ga_{10.5}O_{35.25}$
Space group	*F*23 (196)	*F*432 (209)
Unit cell axis: *a* (Å)	15.07939(7)	15.0556(1)
Z	4	4
R_F^2, R_p, R_{wp}	0.0458, 0.0485, 0.0659	0.0346, 0.0601, 0.0794
χ^2	1.88	2.82

Table 3
Atomic coordinates and atomic displacement parameters for $Ca_{14}Zn_6Ga_{10}O_{35}$

Atom	Position	*x*	*y*	*z*	U_{iso} ($\times 100$ (Å^2))
Ca1	24*f*	0.21338(8)	0.0	0.0	0.67(5)
Ca2	16*e*	0.6122(1)	0.6122(1)	0.6122(1)	0.37(8)
Ca3	16*e*	0.3868(1)	0.3868(1)	0.3868(1)	0.04(7)
M1	16*e*	0.17353(5)	0.17353(5)	0.17353(5)	0.69(4)
M2	16*e*	0.85447(6)	0.85447(6)	0.8545(6)	2.83(6)
M3	4*a*	0.0	0.0	0.0	0.89(8)
M4	24*d*	−0.0010(1)	0.25	0.25	0.32(2)
M5	4*b*	0.5	0.5	0.5	1.24(8)
O1	4*c*	0.25	0.25	0.25	0.97(7)
O2	24*f*	0.3653(2)	0.0	0.0	0.97(7)
O3	16*e*	−0.0684(2)	−0.0684(2)	−0.0684(2)	0.97(7)
O4	48h	0.0679(3)	0.2551(4)	0.3595(4)	0.97(7)
O5	48*h*	0.1550(3)	0.2511(3)	0.5698(3)	0.97(7)

Table 4
Selected interatomic distances (Å) in $Ca_{14}Zn_6Ga_{10}O_{35}$

Ca1	
O2	2.291(4)
O3 ($\times 2$)	2.628(1)
O4 ($\times 2$)	2.400(5)
O5 ($\times 2$)	2.618(5)
Ca2	
O2 ($\times 3$)	2.417(2)
O5 ($\times 3$)	2.283(5)
Ca3	
O2 ($\times 3$)	2.436(2)
O4 ($\times 3$)	2.283(5)
M1	
O1	1.997(1)
O4 ($\times 3$)	1.987(5)
M2	
O3	2.014(6)
O5 ($\times 3$)	1.937(4)
M3	
O3 ($\times 4$)	1.787(6)
M4	
O4 ($\times 2$)	1.952(5)
O5 ($\times 2$)	1.756(5)
M5	
O2 ($\times 6$)	2.031(4)

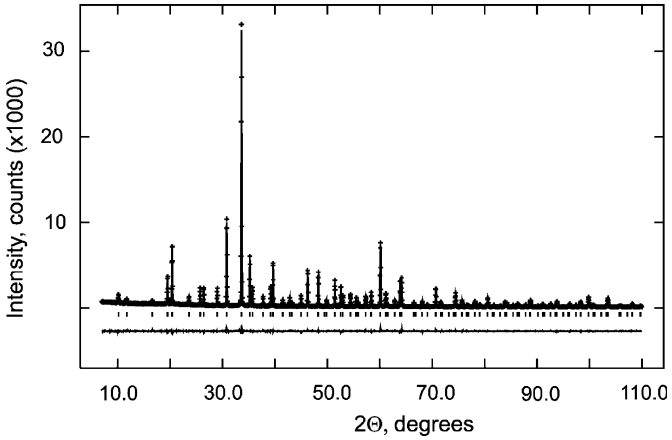

Fig. 2. Observed, calculated and difference X-ray diffraction profiles for $Ca_{14}Zn_6Ga_{10}O_{35}$.

Observed, calculated and difference X-ray diffraction profiles for $Ca_{14}Zn_6Ga_{10}O_{35}$ are shown in Fig. 2.

3.2. The crystal structure of $Ca_{14}Zn_{5.5}Ga_{10.5}O_{35.25}$

During the refinement of the crystal structure of $Ca_{14}Zn_{5.5}Ga_{10.5}O_{35.25}$ models 1 and 2 mentioned above were tested as well. Model 1 led to high reliability factors $\chi^2 = 4.85$, $R_F^2 = 0.11$, $R_p = 0.0748$ while model 2 gave better reliability factors (Table 2). Since partial substitution of Zn^{2+} by Ga^{3+} is accompanied by insertion of O^{2-} ions in the structure as charge compensation, the additional amount of O-atoms calculated based on the cation composition has to be equal to 0.25. These extra oxygen atoms were placed at the O1 position. Refinement of the occupancy of O1 position led to the occupancy of $g(O1) = 0.60(2)$ to be compared with ideal value of $g(O1) = 0.625$. Successive refinement of ADP for oxygen at O1 and its occupancy lead to the reasonable values of $U = 0.006(4)$ Å^2 and $g = 0.61(2)$. However, refinement of the crystal structure with occupancy of O1 fixed at 0.5, led to negative ADP of $U = -0.021(4)$ Å^2. It has to be mentioned that *R*-values remained nearly unchanged during these refinements. Because of the low reliability of the results of refinement of oxygen positions using X-ray powder diffraction data, at the final stages occupancy of the O1 position was fixed to 0.625 and ADPs for the partially occupied oxygen atoms were fixed to $U = 0.025$ Å^2.

Final atomic coordinates and displacement parameters are given in Table 5. Selected interatomic distances are presented in Table 6. Observed, calculated and difference XRD profiles are shown in Fig. 3.

3.3. Impedance spectroscopy studies

Equivalent circuit representation was used for the analysis of the impedance data. Models for the evaluation of the experimental impedance data were the same for both

Table 5
Atomic coordinates, atomic displacement parameters and occupancies of the atomic positions for $Ca_{14}Zn_{5.5}Ga_{10.5}O_{35.25}$

Atom	Position	x	y	z	U_{iso} (× 100 (Å^2))	Occupancies
Ca1	24*e*	0.2114(1)	0.0	0.0	2.02(6)	1.0
Ca2	32*f*	0.38806(6)	0.38806(6)	0.38806(6)	1.53(6)	1.0
M1	32*f*	0.1726(1)	0.1726(1)	0.1726(1)	2.95(5)	0.637(3)
M2	32*f*	0.1422(2)	0.1422(2)	0.1422(2)	1.56(5)	0.363(3)
M3	4*a*	0.0	0.0	0.0	2.31(10)	1.0
M4	24*d*	0.0	0.25	0.25	1.94(4)	1.0
M5	4*b*	0.5	0.5	0.5	0.53(9)	1.0
O1	8*c*	0.25	0.25	0.25	2.50	0.625
O2	24*e*	0.3681(3)	0.0	0.0	1.31(8)	1.0
O3	32*f*	0.0711(4)	0.0711(4)	0.0711(4)	2.50	0.5
O4	96*j*	0.2450 (2)	0.1472(2)	0.0701(2)	1.31(8)	1.0

Table 6
Selected interatomic distances (Å) in $Ca_{14}Zn_{5.5}Ga_{10.5}O_{35.25}$

Ca1	
O2	2.359(5)
O4 (× 4)	2.506(3)
O3 (× 4)	2.599(1)
Ca2	
O4 (× 3)	2.306(4)
O2 (× 3)	2.402(1)
M1	
O1	2.018(3)
O4 (× 3)	1.928(3)
M2	
O3 (× 1)	1.85(1)
O4 (× 3)	1.893(4)
M3	
O3 (× 8)	1.855(9)
M4	
O4 (× 4)	1.875(3)
M5	
O2 (× 6)	1.986(5)

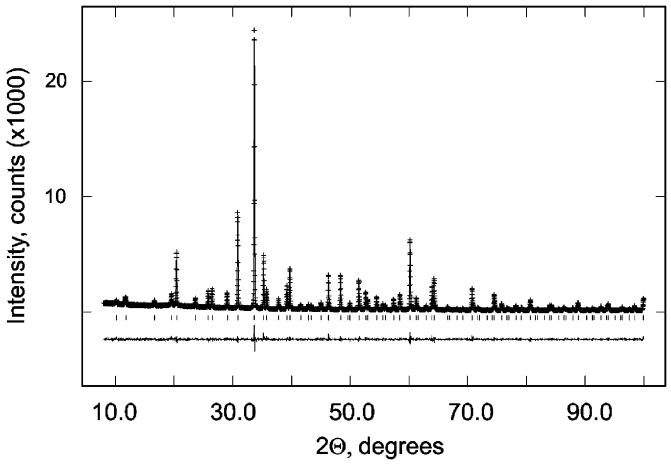

Fig. 3. Observed, calculated and difference X-ray diffraction profiles for $Ca_{14}Zn_{5.5}Ga_{10.5}O_{35.25}$.

$Ca_{14}Zn_{5.5}Ga_{10.5}O_{35.25}$ and $Ca_{14}Zn_6Ga_{10}O_{35}$ (see insets in Fig. 4). C_g in equivalent circuit is added to take into account capacitance of the capacitor formed by platinum electrode and surface of the oxide under investigation. Total conductivity of the polycrystalline samples can be represented by a combination of bulk and grain boundary conductivities. This corresponds to the serial connection of bulk (R_b) and grain boundary resistance (R_{gb}) in equivalent circuit. High capacity of the grain boundaries is expected because of their low thickness. However, due to the possible high dispersion of the grain parameters, constant-phase element (CPE1), instead of capacitor, was placed parallel to R_{gb}.

The correspondence between experimental Nykvist plots and fitted curves obtained with the equivalent circuit shown in the inset of Fig. 4 is satisfactory for the whole studied frequency and temperature ranges. Capacity C_g is nearly constant ($9 \pm 1 \times 10^{-12}$ F) in all the experiments. Phase angle shift of CPE1 ($(0.85–1) \times \pi/2$) is close to the expected capacitive value ($\pi/2$). This indicates low dispersion of the grain boundary parameters. Calculated grain boundary capacity is 7×10^{-11} F and corresponds to the expected geometrical capacity of the grain boundaries.

Temperature dependences of the effective grain boundary (σ_{gb}) and bulk conductivities (σ_b) of $Ca_{14}Zn_{5.5}Ga_{10.5}O_{35.25}$ and $Ca_{14}Zn_6Ga_{10}O_{35}$ are linear in $\log(\sigma T) - 1/T$ coordinates (Fig. 5). Corresponding activation energies of grain boundary ($E_{gb} = 1.80(5)$ eV) and bulk conductivities ($E_b = 1.02(5)$ eV) are within e.s.d. the same for both compounds. One of the explanations for the higher value of E_{gb} in comparison with E_b, could be a variation of the chemical composition on the grain boundary due to the admixtures segregation. Higher bulk conductivity (σ_b) of $Ca_{14}Zn_{5.5}Ga_{10.5}O_{35.25}$ in comparison with $Ca_{14}Zn_6Ga_{10}O_{35}$ (2.1×10^{-5} and 5.8×10^{-6} S/cm at 935 °C, respectively) is likely due to the different defect concentration.

Study of the dependence of the conductivity of the prepared compounds on oxygen pressure performed at 935 °C showed that conductivity values are invariable in the oxygen pressure range 1.6×10^{-4}–0.2 atm.

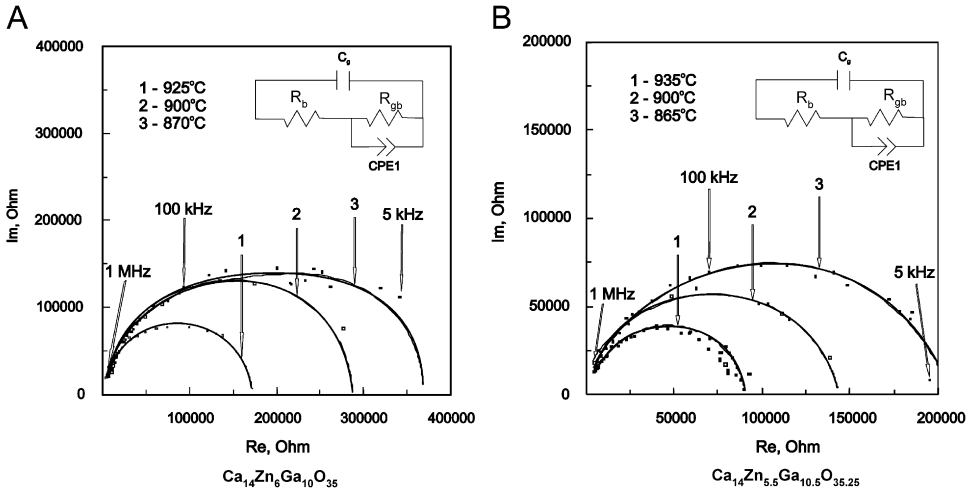

Fig. 4. Complex impedance plane plots for $Ca_{14}Zn_6Ga_{10}O_{35}$ (A) and $Ca_{14}Zn_{5.5}Ga_{10.5}O_{35.25}$ (B) in air at different temperatures. Equivalent circuits are given in insets.

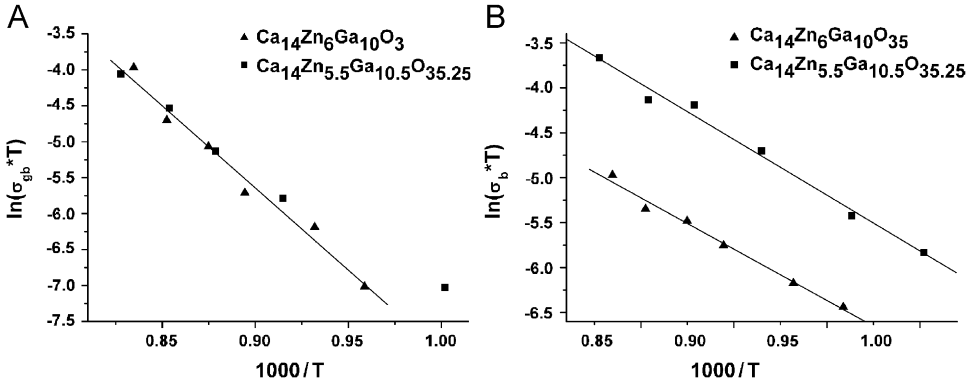

Fig. 5. Temperature dependences (Arrhenius plots) of the effective grain boundary (σ_{gb}) (A) and bulk conductivities (σ_b) (B) of $Ca_{14}Zn_{5.5}Ga_{10.5}O_{35.25}$ and $Ca_{14}Zn_6Ga_{10}O_{35}$.

From the results of the impedance spectroscopy one can conclude that nature of the electrical conductivity in both compounds is similar. Low conductivity values and the absence of the grain boundary effects indicate the lack of noticeable oxide-ion conductivity in both $Ca_{14}Zn_6Ga_{10}O_{35}$ and $Ca_{14}Zn_{5.5}Ga_{10.5}O_{35.25}$.

4. Discussion

The ordered compound $Ca_{14}Zn_6Ga_{10}O_{35}$ is isostructural to $Ca_{14}Zn_6Al_{10}O_{35}$ [3]. There are four tetrahedral and one octahedral sites for Zn/Ga in the crystal structure. As discussed by Grins et al. [1], there are two types of tetrahedra groups in the crystal structure of $Ca_{14}Zn_6Ga_{10}O_{35}$. The first group (group I) represents tetrahedra with the cations M2–M4. Each oxygen of this group is shared between two Zn/Ga cations. These tetrahedra form a 3D network with two types of large empties. One type of these empties is filled with $M5O2_6$-octahedra, centered at 4*b* (1/2,1/2,1/2), while the other ones are occupied by a second unit (group II) consisting of four corner-linked tetrahedra $M1(O1)(O4)_3$ sharing common oxygen atom O1 (Fig. 6). These latter groups are connected with the tetrahedra of group I via the $M4(O4)_2(O5)_2$ tetrahedron. However, only half of the second type of empties is occupied by the group II tetrahedra. They are centered at 4*d* (3/4,3/4,3/4) while the positions at 4*c* (1/4,1/4,1/4) in S.G. *F*23 are remained unoccupied. This situation is illustrated in Fig. 6, where the positions of group II tetrahedra are shown by dark circles. Light circles indicate empty positions.

Bond valences sum (BVS) calculations performed for the Ca sites in the $Ca_{14}Zn_6Ga_{10}O_{35}$ resulted in values quite close to expected ones: Ca1–1.72; Ca2–2.17; Ca3–2.12. It is not straightforward to estimate any preference of Ga^{3+} or Zn^{2+} for a particular site in this structure using the BVS method. This is due to the random distribution of Zn^{2+} and Ga^{3+} cations in the structure and the low accuracy of the oxygen atom positions as XRD data were used for the refinements. However, one can expect the M1 positions to be mainly occupied by the divalent cation Zn^{2+}. Pauling's rules [6] state that in a group of four vertexes linked MO_4

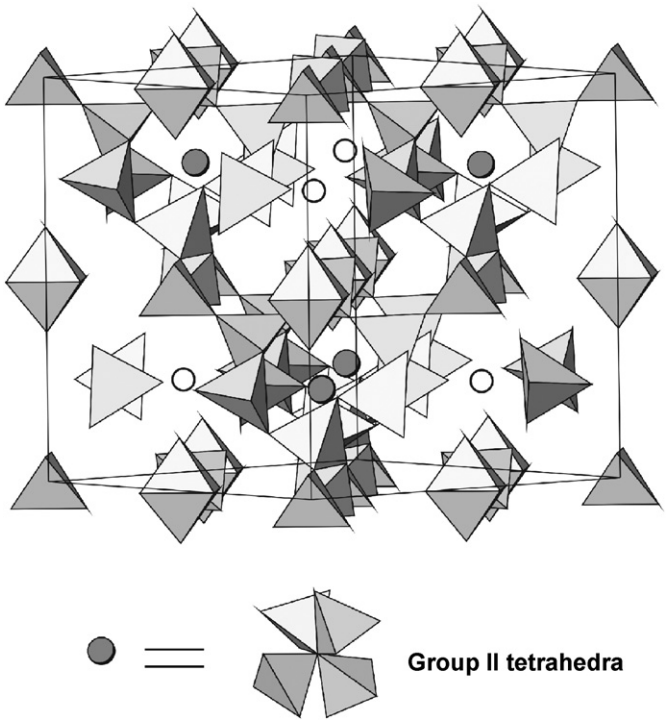

Fig. 6. The crystal structure of $Ca_{14}Zn_6Ga_{10}O_{35}$. Dark circles show positions of group II tetrahedra, while light circles indicate empty positions.

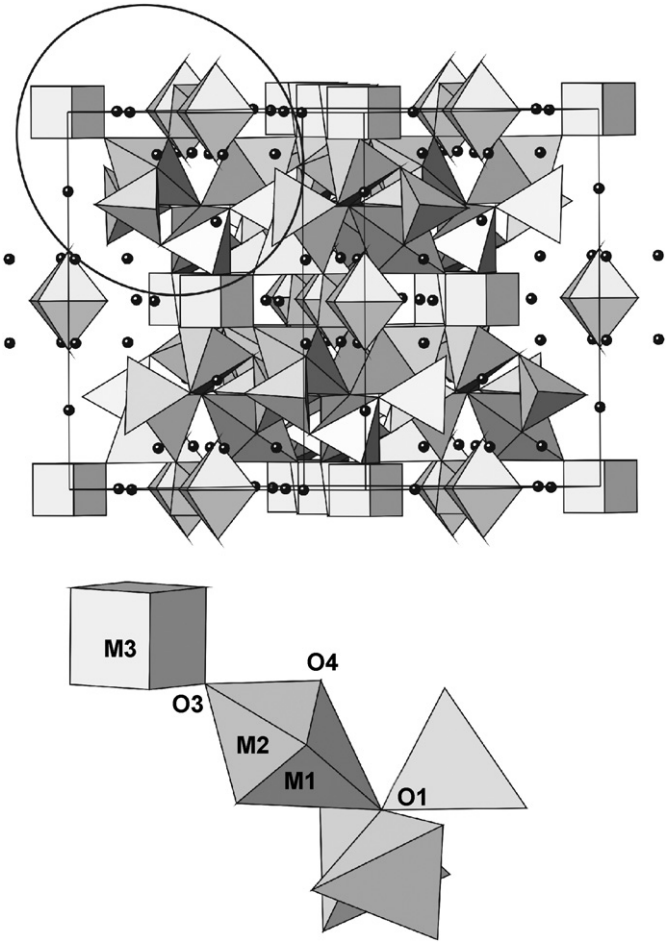

Fig. 7. The crystal structure of $Ca_{14}Zn_{5.5}Ga_{10.5}O_{35.25}$. Magnification of the encircled region is shown on the bottom of the figure.

tetrahedra sharing a common oxygen atom, the M has to be divalent. This is very similar to the situation here where four $M1O1(O4)_3$ tetrahedra share a common oxygen atom, i.e., O1. The $M(1)$ sites should therefore be preferably occupied by the divalent Zn^{2+}. This is supported by the BVS calculation for M1 which gives a value close to 2 (2.07).

Upon partial substitution of Zn^{2+} by Ga^{3+} in $Ca_{14}Zn_{5.5}Ga_{10.5}O_{35.25}$, the oxygen content of the phase has to increase to retain electro-neutrality. The additional oxygen atoms are found in the cavities at the 4*c* (1/4,1/4,1/4) positions in the $Ca_{14}Zn_6Ga_{10}O_{35}$ crystal structure. However, these empty voids are too large for a single oxygen atom as the distance from the center of the voids to the nearest cation is around 2.80 Å. This leads to the peculiar behavior of the crystal structure upon doping. The additional oxygen atom is introduced into the crystal structure as a part of the four tetrahedra groups (group II). Since the total number of $(Zn^{2+}+Ga^{3+})$ cations does not change, a re-distribution of Zn^{2+} and Ga^{3+} in the crystal structure takes place leading to partially occupied tetrahedral sites and accompanying cation disorder.

From the quantity of additional oxygen atoms in $Ca_{14}Zn_{5.5}Ga_{10.5}O_{35.25}$ (0.25), it follows that there is one additional oxygen atom O1 per unit cell. Therefore, the tetrahedral groups II occupy five of eight empty voids in the crystal structure of $Ca_{14}Zn_{5.5}Ga_{10.5}O_{35.25}$ (occupancy of O1 position is 0.625) instead of four found in the crystal structure of $Ca_{14}Zn_6Ga_{10}O_{35}$. As a result, the amount of M1 cations increases while the number of M2 cations decreases. In this case, the ideal occupancies of M1 and M2 positions would be 0.625 and 0.375 to be compared with refined occupancies 0.637(3) and 0.363(3), respectively. The cation deficiency at the $M(2)$ site and the absence of enough M2 cations to bind all of the O3 oxygen atoms, leads in turn to the creation of the anion disorder for the oxygen O3, belonging to the $M3O3_4$ tetrahedra. Part of the O3 oxygen atoms become terminal instead of bridging M3 and M2 cations. The polyhedron around the M3 cation now represents a randomly oriented tetrahedra (cube with half-filled vertices) (Fig. 7). A fragment of the crystal structure of $Ca_{14}Zn_{5.5}Ga_{10.5}O_{35.25}$ illustrating these statements is shown in Fig. 7.

In conclusion, due to the presence of large empty voids in $Ca_{14}Zn_6Ga_{10}O_{35}$, they could be partially occupied by additional oxygen atoms upon substitution of Zn^{2+} by Ga^{3+} as in $Ca_{14}Zn_{5.5}Ga_{10.5}O_{35.25}$. Electrical conductivity measurements showed that the mobility of these oxygen ions is negligible since they are introduced into the crystal structure only as a part of four $M1(O1)(O4)_3$ tetrahedra groups.

Acknowledgments

This work was partially supported by RFBR (#05-03-32844). Authors would like to acknowledge Prof. Gunnar Svensson (Stockholm University, Sweden) for valuable comments and Dr. L.S. Leonova, Dr. A.E. Ukshe and Dr. E.A. Astafyev (IPCP RAS, Chernogolovka) for valuable discussions of the impedance spectroscopy results.

References

[1] J. Grins, S.Ya . Istomin, G. Svensson, J.P. Attfield, E.V. Antipov, J. Solid State Chem. 178 (2005) 2197.

[2] A.M. Abakumov, J. Hadermann, A.S. Kalyuzhnaya, M.G. Rozova, M.G. Mikheev, G. Van Tendeloo, E.V. Antipov, J. Solid State Chem. 178 (2005) 3137.

[3] V.D. Barbanyagre, T.I. Timoshenko, A.M. Il'inets, V.M. Shamshurov, Powder Diffract. 12 (1997) 22.

[4] A.C. Larson, R.B. Von Dreele, General structure analysis system (GSAS), Los Alamos National Laboratory Report LAUR 86-748, 2000;
B.H. Toby, J. Appl. Crystallogr. 34 (2001) 210.

[5] D. Johnson, ZView: A Software Program for IES Analysis, Version 2.8, Scribner Associates Inc., Southern Pines, NC, 2002.

[6] I.D. Brown, The chemical bond in inorganic chemistry, The Bond Valence Model, IUCr Monographs on Crystallography, vol. 12, Oxford University Press, 2002.